

Sub-6dB Aluminum Scandium Nitride Acoustic Delay Lines

Shuai Shao^{*†‡}, Zhifang Luo^{*†‡}, and Tao. Wu^{*†‡‡}

Email: shaoshuai@shanghaitech.edu.cn; luozhf@shanghaitech.edu.cn; wutao@shanghaitech.edu.cn

^{*}School of Information Science and Technology, ShanghaiTech University, Shanghai, China

[†]Shanghai Institute of Microsystem and Information Technology, Chinese Academy of Sciences, Shanghai, China

[‡]University of Chinese Academy of Sciences, Beijing, China

^{‡‡}Shanghai Engineering Research Center of Energy Efficient and Custom AI IC, Shanghai, China

Abstract—This work reports an acoustic delay line (ADL) based on aluminum scandium nitride. In order to reduce the fabrication difficulty and AlScN defects at the bottom electrode edges, a floating bottom electrode is utilized in this acoustic delay line design. ADLs are fabricated with up to 200 μm flat delay gap by $\text{Al}_{0.7}\text{Sc}_{0.3}\text{N}$ and AlN thin film. The increase of piezoelectric coefficient resulting from the 30% Sc doping enhances the electromechanical coupling by more than a factor of 2, compared to AlN. This design achieves an insertion loss of sub-6dB without patterned bottom electrodes. With $\text{Al}_{0.7}\text{Sc}_{0.3}\text{N}$ thin film, an insertion loss of 5.8 dB and a fractional bandwidth (FBW) of 6.0% are obtained at 650 MHz. Compared to the same design AlN device, insertion loss reduced by 27% and fractional bandwidth increased by 9%. This design gives an alternative to low-loss ADLs which does not require consideration of alignment between top and bottom layers.

Keywords—Acoustic delay lines (ADLs), Aluminum scandium nitride (AlScN), Aluminum nitride (AlN), Lamb wave, Unidirectional transducers.

I. INTRODUCTION

Acoustic delay lines (ADLs) based on bulk materials such as lithium niobate demonstrates broad applications in RF filtering[1]–[3], Oscillators[4] and sensors[5], [6]. Single-phase unidirectional transducers (SPUDT) based on Aluminum nitride (AlN) have demonstrated low insertion loss (IL) and a tunable wide range delay and fractional bandwidths (FBW)[7]. The sputtered aluminum nitride (AlN) based ADLs can be simply combined with different material platforms, significantly expanding the application prospects of ADLs. Compared to materials commonly used in SPUDTs, AlN has the advantage of compatibility with CMOS processes and higher power capacity.

There has been much work demonstrating the performance enhancement of Sc doping on AlN resonators[8]–[11], energy harvesters[12] and sensors[13]. The appearance of Sc-doped AlN is promising to improve the performance of AlN-based SPUDT. On the one hand, AlScN films with 30% Sc concentration can obtain a d_{33} enhancement of nearly 3 times. On the other hand, AlScN films with a smaller spring constant leading to a larger acoustic impedance difference between the free surface and the metallized surface can enhance the reflection coefficient of UDT cell. The AlScN-based SPUDT ADL has demonstrated lower losses which utilize the IDTs both on bottom and top compared to the AlN[14]. However, AlScN is more difficult to deposit than AlN, and abnormal orientation grains can be generated due to local enrichment of Sc. These grains, which do not contribute to the piezoelectric

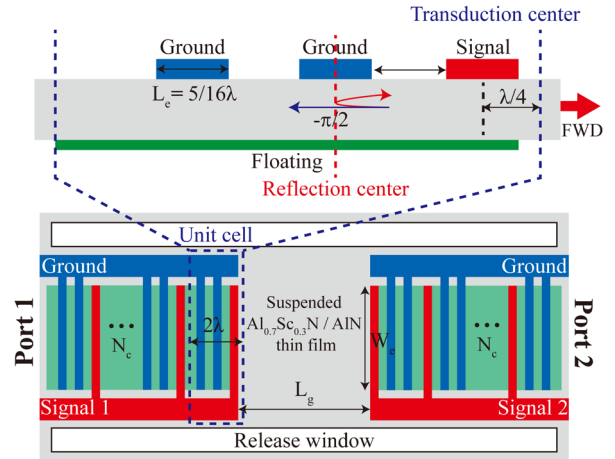


Fig. 1. Schematic of an $\text{Al}_{0.7}\text{Sc}_{0.3}\text{N}/\text{AlN}$ -based SPUDT ADL with floating bottom electrodes. The dimensions of the devices are shown in Table I.

TABLE I DESIGN PARAMETERS OF ALSCN ADLS

Parameters	Value	Parameters	Value
Wavelength λ (μm)	9.6	Electrode width (μm)	3
Number of cells	5	Al thickness (nm)	200
Gap length (μm)	50-200	AlN\AlScN thickness (nm)	1000
Aperture width (μm)	100	Pt thickness (nm)	100

effect, can lead to degradation of device performance. At the same time, these grains will be abundantly present at the edges of the patterned bottom electrode. This work is dedicated to demonstrating an ADL design with lower fabrication difficulties.

In this work, we report the SPUDT ADL based on $\text{Al}_{0.7}\text{Sc}_{0.3}\text{N}$ thin films. By optimizing the sputtering process of the films, high crystalline quality $\text{Al}_{0.7}\text{Sc}_{0.3}\text{N}$ films with a low residual stress are obtained. The S_0 Lamb-wave $\text{Al}_{0.7}\text{Sc}_{0.3}\text{N}$ SPUDT with a gap of 50-200 μm obtained a delay of 11.7-29.9 ns with 3-dB FBW of 6%. The center frequency is 649 MHz and the minimum IL is 5.8 dB. Meanwhile, the velocity of the S_0 lamb wave of the $\text{Al}_{0.7}\text{Sc}_{0.3}\text{N}$ film is extracted as 8604 m/s.

II. ACOUSTIC DELAY LINE DESIGN

The design of the SPUDT is shown in Fig. 1. In order to use both lateral and vertical electric fields to excite the S_0

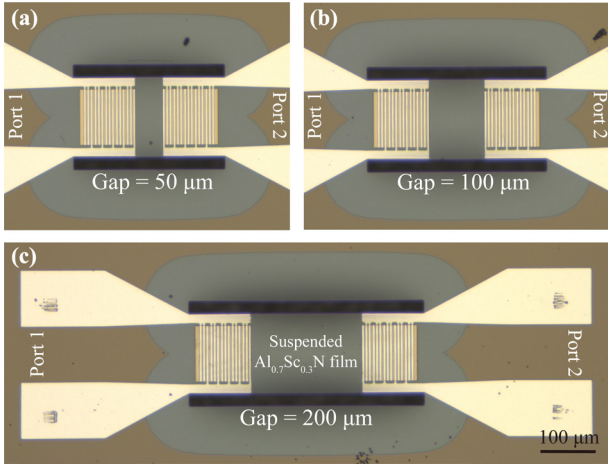


Fig. 2. Optical images of $\text{Al}_{0.7}\text{Sc}_{0.3}\text{N}$ ADLs with gap lengths of (a) $50\ \mu\text{m}$, (b) $100\ \mu\text{m}$ and (c) $200\ \mu\text{m}$.

mode more efficiently, IDTs are arranged above the suspended AlScN film and floating electrodes are arranged below. As shown in Fig 1, the unit cell consists of one signal electrode, two ground electrodes and a bottom floating electrode. The lateral electric field exists between the signal electrode and the adjacent ground electrode, while an alternating vertical electric field exists between the two and the bottom floating electrode. The ground electrode at the edge mainly plays the role of reflection. The right side of the cell is forward direction of the UDT. The length of cells is 2λ . The gap and width of the three pairs of electrodes are $5/16\lambda$. The gap between center of electrodes and the transducer center is $\lambda/4$. The two ground electrodes are set as reflections to produce unidirectionality.

Due to the enhancement of the piezoelectric coefficient of AlN by Sc doping, $\text{Al}_{0.7}\text{Sc}_{0.3}\text{N}$ thin film has 2.8 times the electromechanical coupling coefficient (K^2) of AlN which gives a wider design space to ADLs. Unlike other electrode pairs design for cross-field excitation, floating flat bottom electrodes are used. Flat floating electrodes on one hand avoid alignment between top and bottom electrodes. On the other hand, a large number of defects generated by AlScN grown on the edges of the patterned bottom electrodes have been reported. The flat bottom electrode solves this problem. Low loss and wide bandwidth are obtained due to the use of efficient SPUDT design and $\text{Al}_{0.7}\text{Sc}_{0.3}\text{N}$ thin films. Insertion loss becomes larger as the gap length increases. Since the number of cells is fixed, there is no significant change in fractional bandwidth. The number of cells affects the number of acoustic reflections and the unidirectionality of the transducer, which has an impact on the fractional bandwidth and insertion loss.

III. RESULT AND DISCUSSION

The fabrication process based on $\text{Al}_{0.7}\text{Sc}_{0.3}\text{N}$ of the devices has been reported in [15]. $1\ \mu\text{m}$ thick $\text{Al}_{0.7}\text{Sc}_{0.3}\text{N}$ thin film was deposited using a pulsed DC magnetron reactive sputtering in the EVATEC CLUSTERLINE[®] 200 MSQ with single 4-inch $\text{Al}_{0.7}\text{Sc}_{0.3}$ alloy target. As shown in Table 1, 100 nm Pt was used as the bottom electrode, and the AlScN grown on Pt has better quality, compared to Si and Mo. 200 nm Al for top

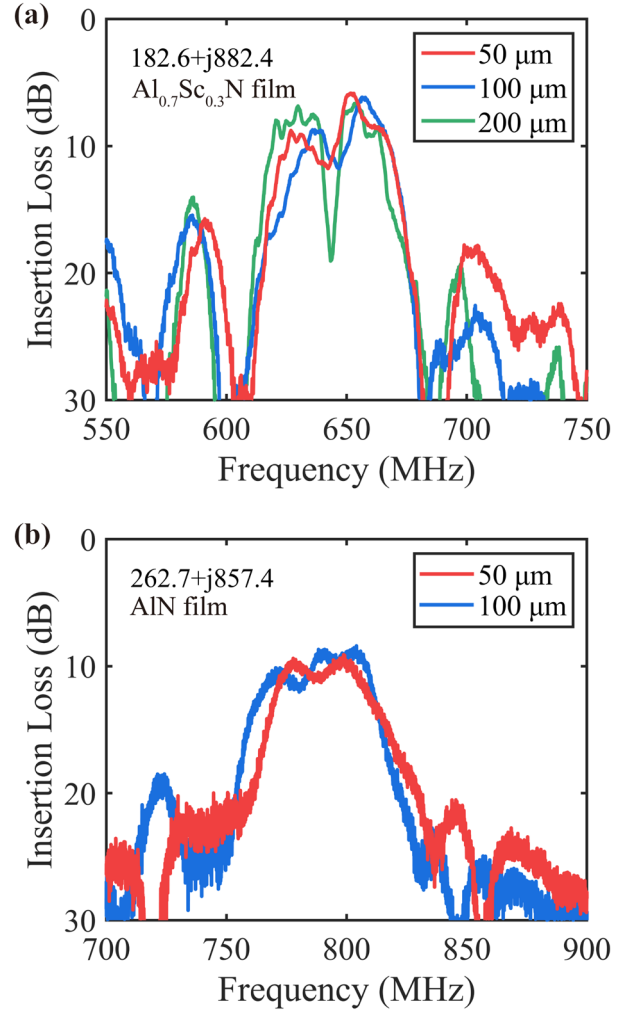


Fig. 3. Measured insertion loss of the 5-cell ADL with different lengths of gaps (50-200 μm). (a) $\text{Al}_{0.7}\text{Sc}_{0.3}\text{N}$, (b) AlN.

electrodes can reduce the resistance of the routing. Figs. 2 (a)-(c) show three fabricated SPUDT ADL with the gap length of $50\ \mu\text{m}$, $100\ \mu\text{m}$ and $200\ \mu\text{m}$, respectively. The design parameters of the devices are shown in Table 1. For comparison, AlN ADLs with the same design and parameters are also fabricated.

Keysight PNA-L N5234B network analyzer with a $200\ \mu\text{m}$ pitch RF probe was used to characterize the device frequency response. Fig. 3 shows the influence of different gap lengths on the insertion loss (IL) of the 5-cell $\text{Al}_{0.7}\text{Sc}_{0.3}\text{N}$ ADLs design with comparison to the same design of AlN devices. As indicated in Fig. 3 (a) and Fig. 3 (b), a minimum IL of 5.8 dB and an FBW of 6.0% were obtained at a gap length of $50\ \mu\text{m}$ with $\text{Al}_{0.7}\text{Sc}_{0.3}\text{N}$ film, while the AlN device shows a minimum IL of 8.0 dB and FBW of 5.5%. The $\text{Al}_{0.7}\text{Sc}_{0.3}\text{N}$ ADLs are matched to $182.6 + j882.4\ \Omega$. Compared to AlN, the 30.5% reduction in the real part significantly reduces the difficulty of impedance matching.

Fig. 4 (a) indicates that the $\text{Al}_{0.7}\text{Sc}_{0.3}\text{N}$ ADL possesses a propagation loss of 11.8 dB/mm. The group delay measured from 50-200 μm gap $\text{Al}_{0.7}\text{Sc}_{0.3}\text{N}$ ADL are 11.7, 21.4 and 29.9 ns, respectively. The extracted group velocity of $1\ \mu\text{m}$ $\text{Al}_{0.7}\text{Sc}_{0.3}\text{N}$ ADL is approximately 8604 m/s as shown in Fig. 4 (b). The group velocity of $\text{Al}_{0.7}\text{Sc}_{0.3}\text{N}$ is lower than the pure AlN due to the lower Young's Modulus with Sc doping,

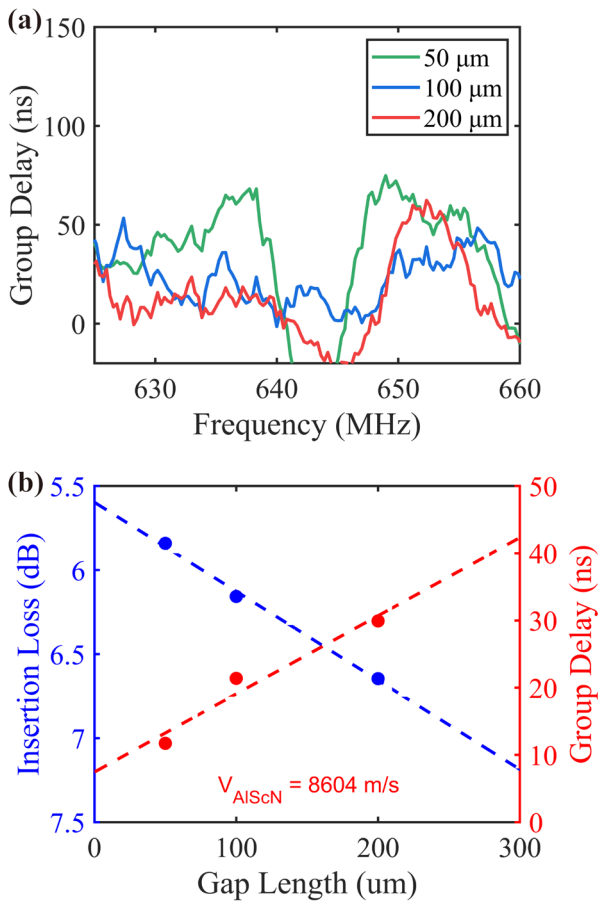


Fig. 4. (a) Group delay with 5-cell $\text{Al}_{0.7}\text{Sc}_{0.3}\text{N}$ ADLs and λ of $9.6 \mu\text{m}$. Gap length varies from $50 \mu\text{m}$ to $200 \mu\text{m}$. (b) Extracted insertion loss.

leading to a relatively longer delay at the same propagation length.

IV. CONCLUSION

In this work, we demonstrate unidirectional $\text{Al}_{0.7}\text{Sc}_{0.3}\text{N}$ ADLs with floating bottom electrodes. The fabricated $\text{Al}_{0.7}\text{Sc}_{0.3}\text{N}$ ADL achieves a low IL of 5.8 dB and an FBW of 6.0 % at a center frequency of approximately 650 MHz. The coupling coefficients improvement by Sc doping enhance the overall performance compared to the AlN ADLs. The extracted group velocity of $\text{Al}_{0.7}\text{Sc}_{0.3}\text{N}$ is 8604 m/s. This work proposes a more easily fabricated ADL design for signal processing and sensing.

ACKNOWLEDGMENT

The authors appreciate the fabrication support from the ShanghaiTech Quantum Device Laboratory (SQDL).

This work was supported in part by the National Natural Science Foundation of China under Grant 61874073, and in part by the Lingang Laboratory under Grant LG-QS-202202-05.

REFERENCES

- [1] J. M. Hode, J. Desbois, P. Difilie, M. Solal, and P. Ventura, "SPUDT-based filters: design principles and optimization," in *Proc. IEEE Int. Ultrason. Symp. (IUS)*, Nov. 1995, pp. 39–50. doi: 10.1109/ULTSYM.1995.495537.
- [2] V. B. Chvets, P. G. Ivanov, V. M. Makarov, and V. S. Orlov, "Low-loss SAW filters using new SPUDT structures," in *Proc. IEEE Int. Ultrason. Symp. (IUS)*, Oct. 1997, pp. 69–72. doi: 10.1109/ULTSYM.1997.662982.
- [3] R. Lu, Y. Yang, S. Link, and S. Gong, "Low-Loss 5-GHz First-Order Antisymmetric Mode Acoustic Delay Lines in Thin-Film Lithium Niobate," *IEEE Trans. Microw. Theory Tech.*, vol. 69, no. 1, pp. 541–550, Jan. 2021, doi: 10.1109/tmtt.2020.3022942.
- [4] M.-H. Li, R. Lu, T. Manzanque, and S. Gong, "Low Phase Noise RF Oscillators Based on Thin-Film Lithium Niobate Acoustic Delay Lines," *J. Microelectromech. Syst.*, vol. 29, no. 2, pp. 129–131, Apr. 2020, doi: 10.1109/JMEMS.2019.2961976.
- [5] W. Wang, K. Lee, I. Woo, I. Park, and S. Yang, "Optimal design on SAW sensor for wireless pressure measurement based on reflective delay line," *Sens. Actuators Phys.*, vol. 139, no. 1, pp. 2–6, Sep. 2007, doi: 10.1016/j.sna.2006.10.018.
- [6] W. Wang, K. Lee, T. Kim, I. Park, and S. Yang, "A novel wireless, passive CO₂ sensor incorporating a surface acoustic wave reflective delay line," *Smart Mater. Struct.*, vol. 16, no. 4, pp. 1382–1389, Jul. 2007, doi: 10.1088/0964-1726/16/4/053.
- [7] R. Lu, S. Link, and S. Gong, "A Unidirectional Transducer Design for Scaling GHz AlN-Based RF Microsystems," *IEEE Trans. Ultrason. Ferroelectr. Freq. Control*, vol. 67, no. 6, pp. 1250–1257, Jun. 2020, doi: 10.1109/tuffc.2020.2968245.
- [8] N. Wang, Y. Zhu, B. Chen, and Y. Zhang, "Over 12% of Coupling Coefficient Demonstrated by 3GHz Sc_{0.12}Al_{0.88}N Based Laterally Coupled Alternating Thickness (LCAT) Mode Resonators," in *Proc. IEEE Int. Ultrason. Symp. (IUS)*, Oct. 2019, pp. 1971–1973. doi: 10.1109/ultsym.2019.8926087.
- [9] G. Esteves *et al.*, "Al_{0.68}Sc_{0.32} N Lamb wave resonators with electromechanical coupling coefficients near 10.28%," *Appl. Phys. Lett.*, vol. 118, no. 17, p. 171902, Apr. 2021, doi: 10.1063/5.0047647.
- [10] S. Shao, Z. Luo, Y. Lu, A. Mazzalai, C. Tosi, and T. Wu, "High Quality Co-Sputtering AlScN Thin Films for Piezoelectric Lamb-Wave Resonators," *J. Microelectromechanical Syst.*, 2022.
- [11] Z. Luo *et al.*, "Al_{0.7}Sc_{0.3}N butterfly-shaped laterally vibrating resonator with a figure-of-merit (kt²·Qm) over 146," *Appl. Phys. Lett.*, vol. 120, no. 17, p. 173508, 2022.
- [12] R. Takei, N. Makimoto, T. Tabaru, M. Akiyama, T. Itoh, and T. Kobayashi, "Scandium aluminium nitride vibration energy harvester with a stress compensation," in *Proc. 19th Int. Solid-state Sens., Acuator Microsyst. Conf. (TRANSDUCERS)*, Jun. 2017, pp. 1879–1882. doi: 10.1109/transducers.2017.7994438.
- [13] J. Su *et al.*, "AlScN-based MEMS magnetoelectric sensor," *Appl. Phys. Lett.*, vol. 117, no. 13, Art. no. 13, Sep. 2020, doi: 10.1063/5.0022636.
- [14] S. Shao, Z. Luo, Y. Lu, A. Mazzalai, C. Tosi, and T. Wu, "Low Loss Al_{0.7}Sc_{0.3}N Thin Film Acoustic Delay Lines," *IEEE Electron Device Lett.*, vol. 43, no. 4, pp. 647–650, Apr. 2022, doi: 10.1109/LED.2022.3152908.
- [15] S. Shao, Z. Luo, and T. Wu, "High Figure-of-Merit Lamb Wave Resonators Based on Al_{0.7}Sc_{0.3}N Thin Film," *IEEE Electron Device Lett.*, vol. 42, no. 9, pp. 1378–1381, Sep. 2021, doi: 10.1109/LED.2021.3100036.